Frequency-dependent interactions determine outcome of competition between two breast cancer cell lines

Audrey R. Freischel[1,2,*], Mehdi Damaghi [1,*], Jessica J. Cunningham[1,2], Arig Ibrahim-Hashim[1],Robert J. Gillies[1], Robert A. Gatenby[1,2], Joel S. Brown[1,2]

[1] Department of Cancer Physiology, [2]Department of Integrated Mathematical Oncology

Moffitt Cancer Center, Tampa, FL

*equal contributions

Correspondence:

Experimental: Mehdi.Damaghi@Moffitt.org

Theoretical: Audrey.Freischel@Moffitt.org

Highlights:

- Demonstrate how mixed-culture spheroids must be used to characterize competition between two cancer cell lines.
- Competition alters growth dynamics of cancer cells.
- Competition growth models can be used to quantify density-independent, density-dependent and frequency-dependent effects on competition.
- Competition affects tumor progression and structure, making it key to understanding tumor development and evolution.

ABSTRACT:

Tumors are highly dynamic ecosystems in which diverse cancer cell subpopulations compete for space and resources. These complex, often non-linear interactions govern continuous spatial and temporal changes in the size and phenotypic properties of these subpopulations. Because intra-tumoral blood flow is often chaotic, competition for resources may be a critical selection factor in progression and prognosis. Here, we quantify resource competition using 3D spheroid cultures with MDA-MB-231 and MCF-7 breast cancer cells. We hypothesized that MCF-7 cells, which primarily rely on efficient aerobic glucose metabolism, would then dominate the population under normoxic conditions; and MDA-MB-231 cells, which exhibit high levels of glycolytic metabolism, would dominate under hypoxic conditions. In spheroids with single populations, MCF-7 cells exhibited equal or superior intrinsic growth rates (density-independent measure of success) and carrying capacities (density-dependent measure of success) when compared to MDA-MB-231 cells in both normoxic and hypoxic conditions. However, when the populations were mixed, MDA-MB-231 cells outcompeted MCF-7 cells under all conditions with competition dynamics determined by frequency-dependent interactions. When grown together, MDA-MB-231 suffered little from MCF-7 while MCF-7 cells experienced a disproportionately large reduction in growth rates in the presence of MDA-MB-231 cells. We frame these results in a game-theoretic (frequency-dependent) model of cancer cell interactions and conclude that competition assays can demonstrate critical density-independent, density-dependent and frequency-dependent interactions that likely contribute to *in vivo* outcomes.

Key Words: cancer cell competition, tumor ecology, tumor evolution, evolutionary therapy

44 **INTRODUCTION:**

45 Each malignant tumor typically contains diverse and heterogeneous habitats due to spatial and temporal
46 variations in cell density, immune infiltration, and blood flow (1-3). Here, we investigate the
47 evolutionary effects of variations in substrate (e.g. glucose, oxygen, and glutamine) and metabolites
48 (e.g. H^+) that are typically governed by alterations in blood flow. These changes, in turn, can alter the
49 local fitness (competitive advantage) of the extant cell populations that can have dramatic evolutionary
50 effects on the phenotypic and genotypic properties of the cancer cells.

51 Recently, two general "niche construction" strategies were observed in clinical and pre-clinical cancers
52 (4, 5). The first consists of cancer cells that possess high levels of aerobic glycolysis that generate an
53 acidic environment which promotes invasion and protects cells from the immune system. These cells are
54 typically invasive and motile. In the second niche construction strategy, cancer cells promote growth by
55 recruiting and promoting blood vessels. This angiogenic phenotype is typically non-invasive and
56 maintains near-normal aerobic metabolism of glucose. These divergent phenotypes can be found within
57 the same tumor (6-9). The invasive "pioneer" phenotype is optimally adapted to survive and thrive at
58 the tumor edge. There it can co-opt normal tissue vasculature as it invades, and its acidic environment
59 provides protection from immune cells at the tumor-host interface. In contrast, the "engineer" cancer
60 cells are well suited to the interior regions of the tumor where their angiogenic phenotype can, with
61 varying degrees of success, provide blood flow necessary to deliver substrate and remove metabolites.
62 When the pioneers and engineers interact, they presumably compete for both space and substrate.
63 However, the specific phenotypic traits that confer maximal fitness under different micro-environmental
64 conditions have not been well established.

65 Competition between two species leads to four possible outcomes: 1) species A outcompetes B, 2) B
66 outcompetes A, 3) A or B outcompetes the other depending upon who establishes first (alternate stable

67 states), or 4) the two species coexist. These population dynamics can be mathematically framed through
68 the Lotka-Volterra equations for inter-specific competition (10, 11). Derived independently by Lotka
69 (1910) and Volterra (1920), the eponymous equations were first tested empirically by Gause (1932) in
70 the, now classic, competition experiments using various species of *Paramecium* and yeast (12, 13). This,
71 and subsequent work on fruit flies, flour beetles, and various natural systems, have confirmed the
72 predictive power of the Lotka-Volterra equations (14, 15). Such assays utilize growth dynamics to
73 elucidate the critical phenotypic properties that determine fitness under different environmental
74 conditions (16).

75 In ecological systems, growth dynamics are divided into three categories: *density dependent* (DD),
76 *density independent* (DI), and *frequency dependent* (FD) effects. Density dependent (DD) effects occur
77 when one cancer cell type outcompetes another because it can achieve a higher equilibrium cell density
78 (carrying capacity) under conditions of space or nutrient limitations. *Density independent* (DI) effects
79 include intrinsic growth rate, which measures the capacity of a cell line to grow exponentially under
80 ideal conditions. In cell biology, these (DD and DI) are often used as indicators of cell fitness (17-19).
81 This, however, ignores the FD interactions which often determine competitive outcomes. Frequency
82 dependent (FD) effects occur when one cell type outcompetes another because its phenotype
83 disproportionately depresses the growth rate of another as a result of more rapid resource uptake, or
84 via direct interference with the other cell type. This game theoretic effect implies that the success of an
85 individual cell is context dependent. It depends not only on the density of other cells around it, but the
86 phenotypes of those cells as well (20, 21). Because of this, FD effects and the outcome of competition
87 can only be evaluated using Gause-style competition assays in which mixtures of the two cell types are
88 grown together using different starting frequencies.

89 Here, we utilize Gause-style competition assays to investigate the competitive interaction between
90 engineer and pioneer phenotypes. These strategies will be represented by the well-characterized MDA-
91 MB-231 and MCF-7 cell lines which are often used as representative of the highly glycolytic and invasive
92 and low glycolytic and non-invasive phenotypes, respectively (22-26). Assays were conducted in 3D
93 spheroid cultures with varying starting frequencies of each cell type. The spheroid system was selected
94 as an *in vitro* intermediate between 2D cell culture, which may reach an equilibrium state through
95 confluence rather than resource competition, and *in vivo* subcutaneous mouse models, which provide
96 less opportunity for replication and frequent monitoring of the two cell populations (27-34). Spheroids
97 were grown in various combinations of pH and glucose concentrations, letting the 3D structure provide
98 natural nutrient and oxygen gradients. Glutamine availability was also varied to test for growth and
99 competition effects due to secondary nutrients.

100 As in the Gause experiments, measures of growth dynamics were used to evaluate competitive ability.
101 DI, DD, and FD effects corresponded to selection for higher growth rates, carrying capacities, and
102 competitive ability, respectively. Carrying capacities (DD) were estimated from monoculture spheroids in
103 varying culture conditions. Initial growth rates (DI) of each cell type were estimated from both mono-
104 and co-cultured spheroids. As FD effects rely on interactions between cell types, their values were
105 estimated using the Lotka-Volterra competition model. In order to remain agnostic to the mode of
106 tumor spheroid growth, our growth model was selected by first fitting monoculture spheroids to four
107 common growth models (exponential, Monod, logistic, and Gompertz), then selecting the model which
108 best approximated the growth of monoculture spheroids in all culture conditions. This model was then
109 expanded to its two-species competition form and used to obtain estimates of competition coefficients
110 for each cell line under eight different nutrient conditions.

111 Based on published experimental studies, we expected both cell types to have higher growth rates and
112 carrying capacities at physiological pH (pH 7.4) and higher nutrient levels. MCF-7 cells, which
113 predominantly use oxidative phosphorylation for metabolism of glucose, was predicted to be
114 significantly inhibited by low pH, while MDA-MB-231 cells, which exhibit the Warburg phenotype with
115 high levels of aerobic glycolysis, was expected to be more tolerant. Because the glycolytic MDA-MB-231
116 cells need more glucose to produce energy compared to the oxygen-consuming MCF-7 cells, we
117 expected the former to respond more favorably to increased glucose concentrations than the latter. We
118 also predicted that, based on their metabolic differences, MCF-7 cells would be fitter under conditions
119 of normal pH and low glucose; and vise-versa for the MDA-MB-231 cells.

120 Herein, we test our hypothesis through competition experiments between the MCF-7 and MDA-MB-231
121 cells under varying environmental conditions. We report the outcome of these competition assays as
122 well as the effect of nutrient availability on DD and DI effects and evaluate their ability to indicate
123 competitive outcome. We used fluorescent measurements to approximate cell growth in the spheroid
124 and propose that the logistic growth equation best approximates the growth of both cell types in the
125 majority of culture conditions. We then used Lotka-Volterra competition equations to determine the
126 contribution of population growth rates (DI), maximal population size (DD) and/or competition
127 coefficients (FD) on the outcome of interspecific competition. Lastly, we compared these results to the
128 outcome of competition between MDA-MB-231 and MCF-7 from mixed tumors *in vivo*.

129

130

131 **RESULTS:**

132 ***MDA-MB-231 out-compete MCF-7 cells under all pH, glucose and glutamine levels, and starting***
133 ***frequencies***

134 Fluorescently labeled MCF-7 (GFP) and MDA-MB-231 (RFP) cells allowed us to non-destructively
135 measure population dynamics within each micro-spheroid. We used this spheroid system to: 1) observe
136 the outcome of competition (mixed culture), 2) compare population growth models (mono-cultures), 3)
137 measure intrinsic growth rates (DI), 4) measure carrying capacities (DD), and 5) determine competition
138 coefficients (FD). In experiments 1 and 2, spheroids started with a plating density of 20,000 and 10,000
139 cells, respectively, with initial conditions of 0%, 20%, 40%, 60%, 80% and 100% MDA-MB-231 cells
140 relative to MCF-7 cells. In experiment 1, additional treatments included neutral (7.4) versus low (6.5) pH
141 and varying levels of glucose (0, 1, 2, 4.5 g/L) (Figure 1B). Experiment 2 had treatments of pH (7.4, 6.5),
142 glucose (0, 4.5 g/L), and glutamine positive and starved media (Figure 1C). Both experiments were
143 further subdivided into parts A and B based on culture conditions (Figure 1 provides details). In
144 experiment 1, microspheres were grown for 670 hours with fluorescence measured every 24-72 hours.
145 In experiment 2, microspheres were grown for 550 hours with fluorescence measured every 6-12 hours.
146 Growth medium was replaced every 4 days without disturbing the integrity of the microsphere.

147

A.

	MCF-7	MDA-MB-231
Source Tissue	*Luminal Epithelium*	*Basal Epithelium*
Cancer Type	*Invasive Ductal Carcinoma*	*Adenocarcinoma*
Receptor Status	*ER+, PR+, EGFR-, HER2-*	*ER-, PR-, EGFR+, HER2-*
Properties	***Strong Cell-Cell Adhesion***	***Weak Cell-Cell Adhesion***
	Non-Invasive	*Invasive*
	Normal Glucose Metabolism	***Upregulated Aerobic Glycolysis***

B.

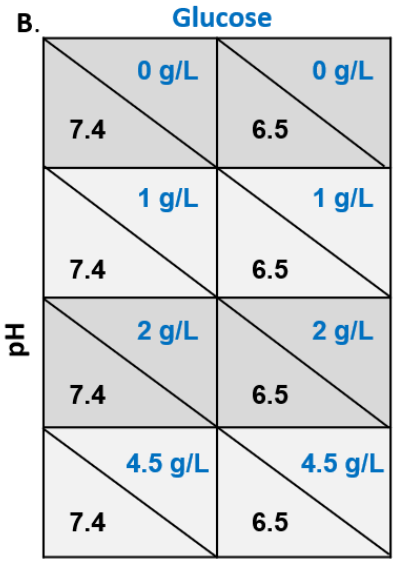

C.

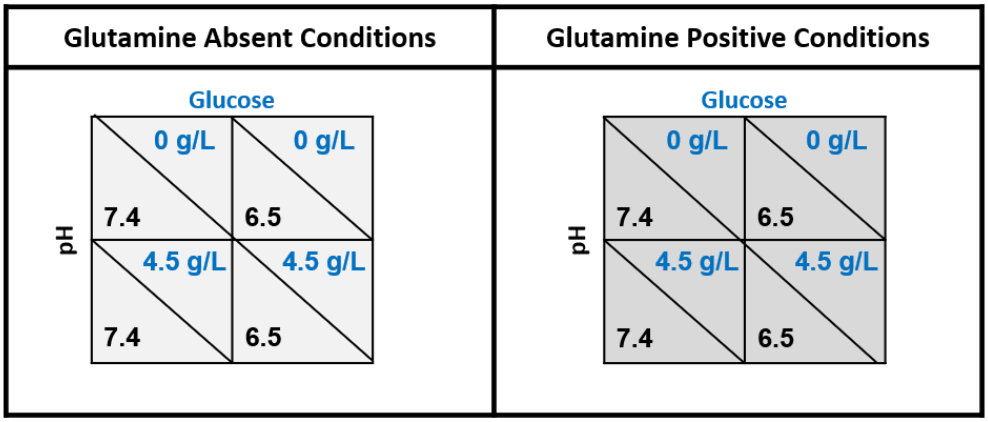

Figure 1: A. Phenotype and source information for the "niche constructing" MCF-7 and the "pioneer" MDA-MB-231 cell lines. **B.** Growth dynamics of monoculture and mixed population tumor spheroids in glucose concentrations of 0 g/L and 2 g/L (experiment 1A, in dark gray) and of 1 g/L and 4.5 g/L (experiment 1B, in light gray) were compared at physiological (7.4) and low (6.5) pH. **C.** Experiment 2 measured the growth dynamics of mixed population tumor spheroids in 4.5 g/L glucose and 0 g/L glucose, in physiological (7.4) and low (6.5) pH, and with (experiment 2A, in dark gray) and without (Experiment 2B, in light gray) glutamine to evaluate differences in growth due to the presence of a secondary nutrient.

157 In mixed cultures and regardless of initial conditions (starting frequencies, pH, glucose and glutamine),
158 MDA-MB-231 outcompeted MCF-7 cells (Figure 2). Contrary to our hypothesis, MCF-7 did not
159 outcompete the MDA-MB-231 cells under conditions of low glucose and neutral pH. This raises the
160 question of whether the success of the MDA-MB-231 was a consequence of higher intrinsic growth
161 rates, increased carrying capacities, or consistently favorable competition coefficients.

162

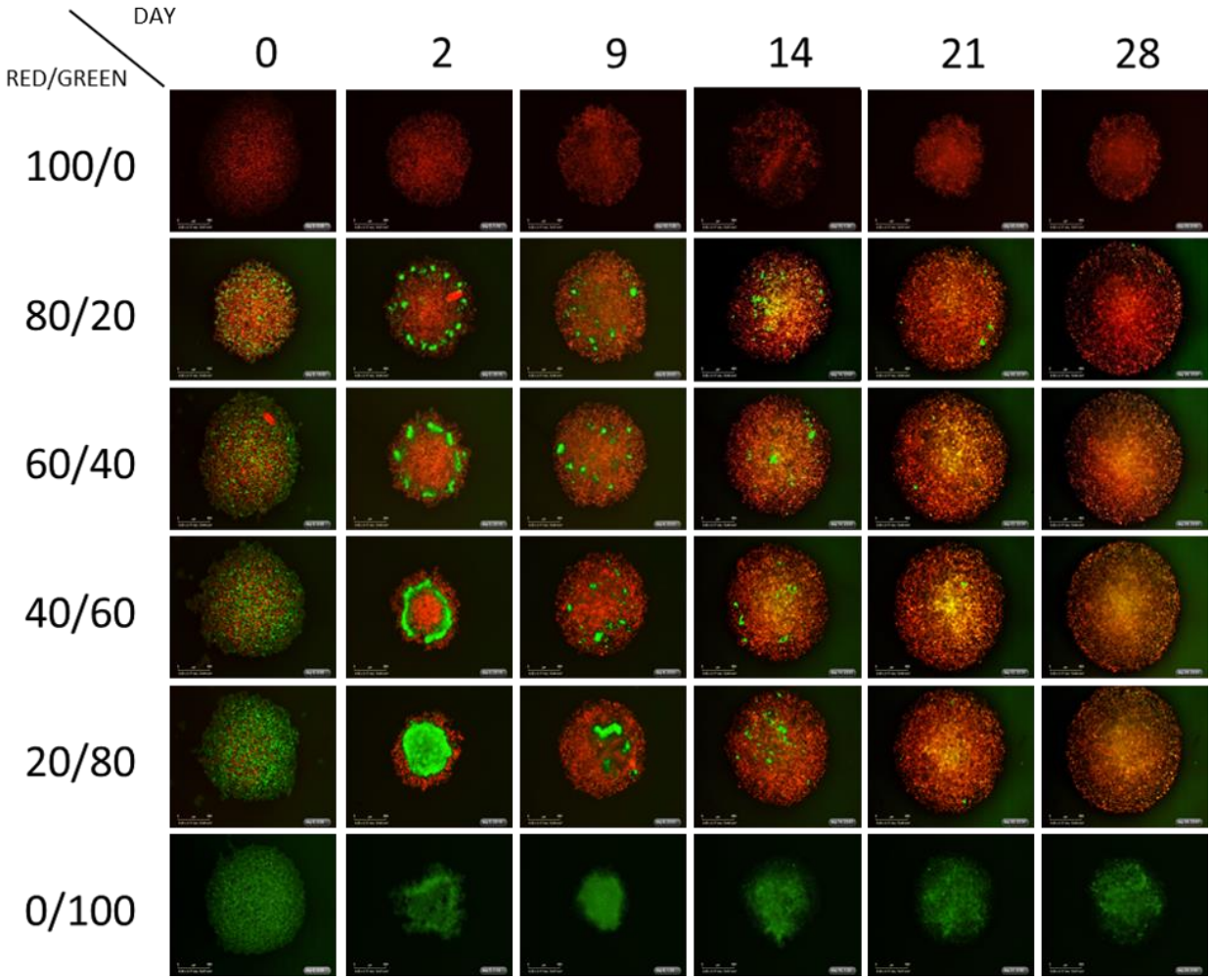

Figure 2: Outcome of competition for all starting frequencies in 2g/L glucose and neutral pH. In all starting conditions, MDA-MB-231 outcompete MCF-7.

166 ***MCF-7 cells have a higher intrinsic growth rate under all culture conditions***

167 In both experiments, MCF-7 cells had similar or significantly higher intrinsic growth rates compared to
168 MDA-MB-231 cells (Figures 3A & 4A). The absence of glutamine reduced the difference in instantaneous
169 growth rates between the two cell types, regardless of pH or glucose concentration (Figure 3A),
170 consistent with its role as a substrate for respiration, which is more pronounced in MCF-7 cells.
171 Separate three-way ANOVAs were performed for the two cell types and experiments 1 and 2 to
172 determine the effects of culture conditions. In these ANOVAs, pH (low versus high), nutrient level
173 (either various glucose of glutamine levels), and starting frequencies of cell types were the independent
174 variables (Supplementary tables 1-4).

175 As expected, the growth rate of MCF-7 cells generally increased with glucose concentration, but pH had
176 little effect. There were some notable significant interaction effects between glucose and pH. In
177 experiment 1A, growth rates decreased with pH in the absence of glucose and increased with pH in the
178 presence of glucose. In experiment 1B, growth rates did not vary with pH at low glucose (1g/L) but
179 showed a notable and unexpected decline with pH at high glucose (4.5 g/L). In experiment 2, the
180 exception to increasing growth rates with increased pH and glucose occurred for glutamine positive,
181 neutral pH conditions. In this case, growth rates declined with glucose. Growth rates did not vary
182 significantly with glucose concentration or pH in the presence of glutamine. In the absence of glutamine,
183 the growth rate of MCF-7 cells significantly increased with increased pH and this effect was amplified in
184 the absence of glucose.

185 Unexpectedly, the growth rates of MDA-MB-231 tended to decline with glucose. In experiment 1A and
186 1B, growth rates decreased significantly with glucose concentration and increased with pH. In
187 experiment 2A, growth rates also declined significantly with glucose. The effect of pH was dependent
188 on the presence of glutamine. With glutamine, growth rates declined with pH (higher under acidic

189 conditions) and, without glutamine they increased with pH. It may be that glucose is less an essential
190 nutrient than a nutrient used to gain a competitive edge on one's neighbors. We will elaborate more on
191 this counter-intuitive result in the discussion.

192 The initial frequencies of cell types had revealing effects on the instantaneous growth rates. In all
193 experiments, both cell types had lower growth rates as the frequency of MDA-MB-231 increased (Figure
194 3C & 4C). In experiment 2, when there is glutamine present, starting frequency is the only variable which
195 significantly affected growth rates. At the lower starting densities (experiment 2) in the presence of
196 glucose, MCF-7 cells show an increase and then a sharp decline (at 80%) as the frequency of MDA-MB-
197 231 cells in the starting population increased. In general, under all culture conditions, both cell types
198 have slower initial growth rates with increasing starting frequency of MDA-MB-231. In summary, the
199 higher intrinsic growth rate of MCF-7 cells (DI effects) does not predict which cell type outcompetes the
200 other.

201 ***MCF-7 cells have a higher Carrying Capacity in all culture conditions***

202 In both experiments, the MCF-7 cells reached the same or significantly higher carrying capacities than
203 MDA-MB-231 (Figures 3B & 4B). For both cell types, in the presence of glutamine, carrying capacities
204 increased with glucose in neutral pH conditions. Surprisingly, the MCF-7 cells experienced a decrease in
205 carrying capacity with increasing pH, whereas the MDA-MB-231 experienced an increased carrying
206 capacity with pH. This was observed regardless of glutamine status. The only exception to this behavior
207 was in acidic (2g/L glucose, 6.5 pH with glutamine) conditions, where the MCF-7 cells had a depressed
208 carrying capacity.

209 MDA-MB-231 carrying capacities appeared more sensitive to culture conditions than those of MCF-7. In
210 the presence of glutamine, their carrying capacity increased significantly with pH. Their carrying capacity
211 increased with glucose up to concentrations of 2g/L but becomes suppressed in high (4.5g/L)

212 concentrations of glucose. Experiment 2 showed this effect of glucose regardless of glutamine status. In

213 summary, the carrying capacities (DD effects) also do not predict which cell type outcompetes the other.

214

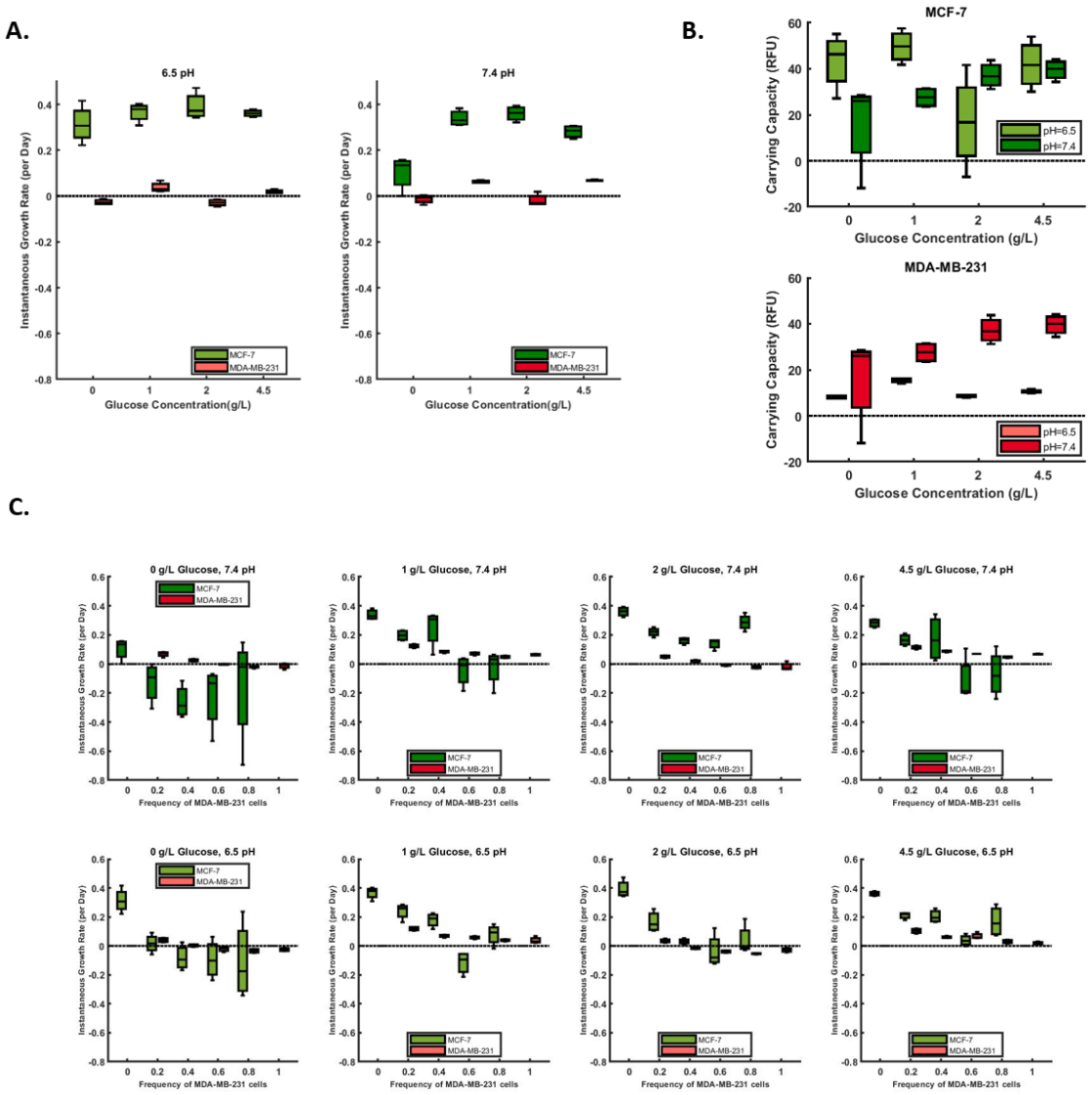

Figure 3: Growth estimates of mixed population tumor spheroids for experiment 1. **A.** Instantaneous growth rate (per day) for each cell type in high and low pH at various glucose concentrations. **B.** Carrying capacities (in Relative Fluorescent Units (RFU), measured as the average fluorescence in the last ten experimental time points) for each cell type in high and low pH at various glucose concentrations. **C.** Instantaneous growth rate (per day) of each cell type in different starting frequencies for all eight culture conditions.

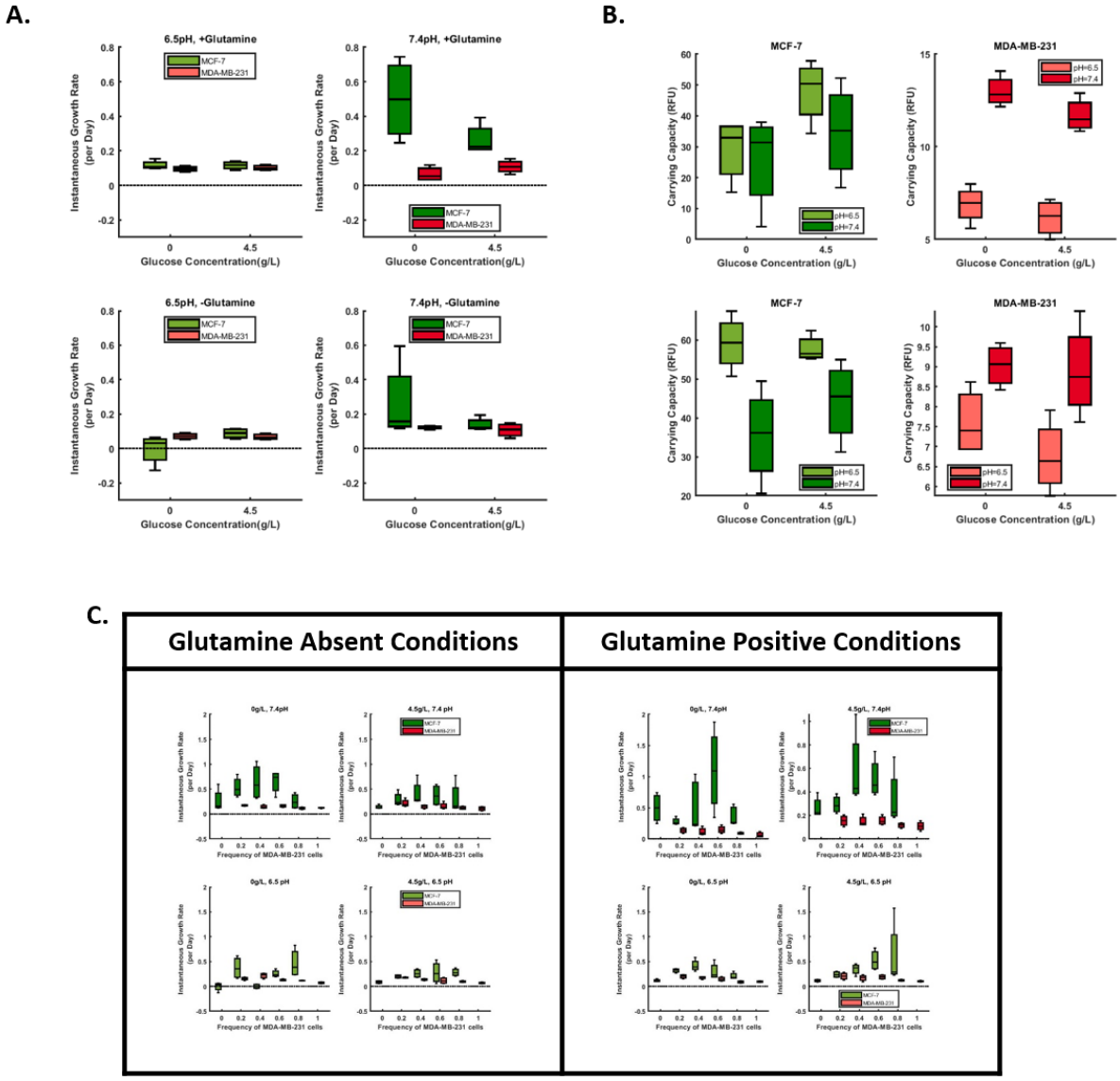

Figure 4: Growth estimates of mono-culture population tumor spheroids for experiment 2. **A.** Instantaneous growth rate of MCF-7 (green) and MDA-MB-231 (red) cells in nutrient rich and nutrient deficient conditions. **B.** Carrying capacity of MCF-7 and MDA-MB-231 cells in nutrient rich and nutrient deficient conditions. **C.** Instantaneous growth rate (per day) of each cell type in different starting frequencies for all eight culture conditions.

228 ***The Logistic Model Best Describes Individual Cell Growth***

229 Frequency-dependent effects (here measured as competition coefficients) can only be quantified by
230 modelling the growth of multiple interacting types or species. In order to obtain an accurate estimate of
231 these, the mode of growth must first be determined. Although several growth models have been
232 proposed for spheroids, tumors, and organoids, no specific consensus has been reached (35, 36).
233 Because of this, we agnostically compared four population growth models: exponential, logistic,
234 Gompertz, and Monod-like.

235 The exponential growth model is commonly used in bacterial studies and assumes unlimited resources
236 (37). This was used as a null model which allowed us to confirm that our spheroid cultures experience
237 limits to growth. Logistic population growth is the simplest constrained growth model and assumes that
238 per capita population growth rate declines linearly with population size or density (38). Although it
239 gives a similar shape, Gompertz growth is exponentially constrained by increasing population. Several
240 authors and works have suggested that the Gompertz equation provides a better fit to the growth of
241 tumors *in vivo* (36, 39). The Monod-like equation imagines resource matching where per capita growth
242 rates are proportional to the amount of resources supplied per individual. It provides a good fit to the
243 population growth curves of bacteria and other single cell organisms grown in chemostats (40). Here,
244 we consider all four models when estimating the DI parameter of intrinsic growth rate (r). We used the
245 latter three models for estimating the DD parameter of carrying capacity (K).

246 Due to the increased number of time points, we used the experiment 2 mono-culture spheroids to fit
247 the four models of single cell-type population growth. Using ordinary least squares approach, all four
248 models were fit to the four replicate spheroids of MCF-7 or MDA-MB-231 cells under eight
249 environmental conditions (Supplementary Figure 1). Quality of fit for each model was evaluated using
250 adjusted R^2 and Root Mean Square Error (RMSE) (Table 1, Supplementary Table 5).

Model	Cell Line	Measure	4.5 g/L Glucose, 7.4 pH, +Glutamine	4.5 g/L Glucose, 7.4 pH, -Glutamine	4.5 g/L Glucose, 6.5 pH, +Glutamine	4.5 g/L Glucose, 6.5 pH, -Glutamine	0 g/L Glucose, 7.4 pH, +Glutamine	0 g/L Glucose, 7.4 pH, -Glutamine	0 g/L Glucose, 6.5 pH, +Glutamine	0 g/L Glucose, 6.5 pH, -Glutamine
Exponential	MCF-7	Adjusted R^2	0.86375925	0.986878377	0.981146959	0.948234222	0.878382763	0.988394753	0.680927938	0.862338251
		RMSE	4.350169084	1.132653242	1.69847635	3.695432283	3.27179314	1.075082735	2.671205198	8.252546774
	MDA-MB-231	Adjusted R^2	0.965940219	0.961195759	0.405939888	0.837579643	0.984098581	0.920137544	0.673358471	0.792081228
		RMSE	0.464566345	0.395146745	0.808032208	0.430099077	0.389104518	0.495043084	0.684053081	0.61219965
Logistic	MCF-7	Adjusted R^2	0.95109814	0.987162238	0.981296804	0.948907945	0.989835743	0.990746769	0.706812568	0.954187534
		RMSE	2.569889623	1.119624296	1.693018458	3.678532642	0.920541516	0.955498916	2.560276438	5.403291938
	MDA-MB-231	Adjusted R^2	0.96590504	0.984894861	0.912214515	0.956642704	0.984068806	0.961748527	0.975726308	0.917447748
		RMSE	0.464826241	0.244756935	0.311220709	0.221858188	0.389432857	0.341782758	0.186174247	0.385055441
Monod	MCF-7	Adjusted R^2	0.931940694	0.970120375	0.927134074	0.865196707	0.96774423	0.944005043	0.715360107	0.784133576
		RMSE	3.027431032	1.708127542	3.338320975	5.959270988	1.669117432	2.349660049	2.522459912	11.38349256
	MDA-MB-231	Adjusted R^2	0.942552982	0.987666692	0.874817759	0.962825606	0.939280229	0.972592786	0.965887218	0.921638951
		RMSE	0.603401178	0.221046584	0.370619137	0.205360395	0.759417203	0.288935986	0.220623679	0.375119346
Gompertz	MCF-7	Adjusted R^2	0.943527504	0.987314557	0.981080261	0.948061608	0.985336984	0.990179344	0.711173682	0.945493131
		RMSE	2.760461987	1.112887278	1.702046991	3.705015484	1.111112845	0.983955476	2.540994298	5.737193572
	MDA-MB-231	Adjusted R^2	0.965812133	0.986346591	0.896293181	0.960341196	0.983941859	0.967290012	0.972497979	0.920364898
		RMSE	0.465418306	0.232605999	0.337719056	0.212122131	0.39072316	0.315765537	0.198161845	0.378158388

Table 1: Average adjusted R2 and RMSE for OLS fitting of four growth models to monoculture spheroids in experiment 2. Although similar to the Gompertz fits, the Logistic Growth model provided the lowest RMSE for most culture conditions.

255 Two-way ANOVAs (one for each cell type with pH and nutrient levels as independent variables) showed
256 that adjusted R^2's were similar for the three density-dependent models and significantly lower for the
257 exponential model (Supplementary Table 6). Conversely, the RMSE indicated the best fit for exponential
258 growth (lowest value), lowest quality fit for the Monod-like equation, and similar, intermediate values
259 for the logistic and Gompertz growth models. To definitively reject the (null) exponential model, we
260 evaluated whether the spheroids reached carrying capacity. To do this, we examined the slope of the
261 final ten time points for both the red and green fluorescent values (RFU's) for all experiment 2 spheroids
262 (supplementary table 7). As both MCF-7 and MDA-MB-231 mono-culture spheroids showed near, or
263 approaching, zero slopes, we rejected the exponential growth model. This was further confirmed by
264 two-way ANOVA (Supplementary table 8). Lastly, the Gompertz, Logistic, and Monod-like models were
265 directly compared and found to have significantly different RMSEs (supplementary table 9). Of these,
266 the Logistic model had the lowest RMSE, thus, it provided the best fit for our data.

267 ***MDA-MB-231 cells have a competitive advantage over MCF-7 cells in all culture conditions***

268 The Lotka-Volterra competition equations represent a two species extension of logistic growth with the
269 addition of competition coefficients.

270
$$\frac{dN_1}{dt} = N_1 r_1 \left(1 - \frac{N_1 + \alpha N_2}{K_1}\right)$$

271
$$\frac{dN_2}{dt} = N_2 r_2 \left(1 - \frac{N_2 + \beta N_1}{K_2}\right)$$

272 where N_i are population sizes, r_i are intrinsic growth rates and K_i are carrying capacities. We let species
273 1 and 2 be MCF-7 and MDA-MB-231, respectively. The competition coefficients (α and β) scale the
274 effects of inter-cell-type competition where α is the effect of MDA-MB-231 on the growth rate of MCF-7
275 in units of MCF-7, and vice-versa for β. If α (or β) is close to zero, then there is no inter-cell-type

276 suppression; if α (or β) is close to 1 then intra-cell-type competition and inter-cell-type competition are
277 comparable; and if α (or β) is >1 then inter-cell-type competition is severe.

278 To fit this model, we used the time series data from experiment 2. The population sizes of the four
279 replicate spheroids were averaged for each of the eight environmental conditions and starting initial
280 frequencies of both cell types. Using the ordinary least squares approach, we estimated the values for
281 instantaneous growth rates, carrying capacities, and competition coefficients α and β (Figure 5). Note
282 that this gives revised estimates for growth rates and carrying capacities in addition to measuring the
283 competition coefficients.

284

A.

+ Glutamine

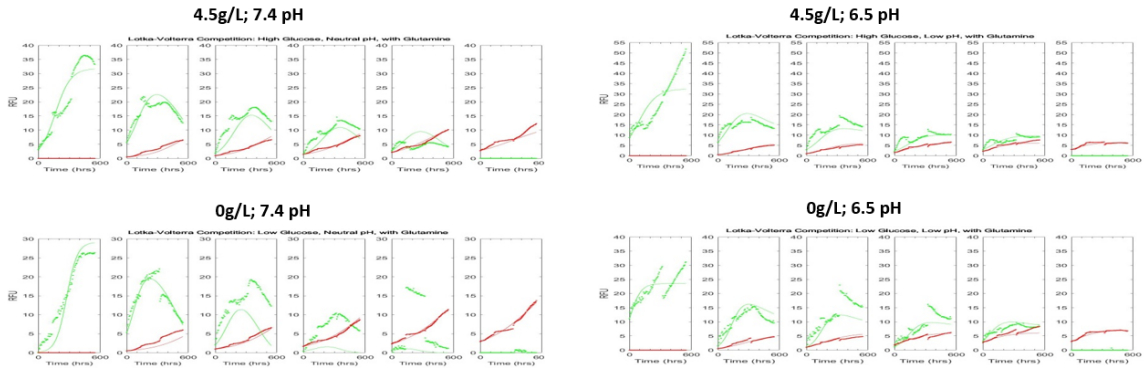

- Glutamine

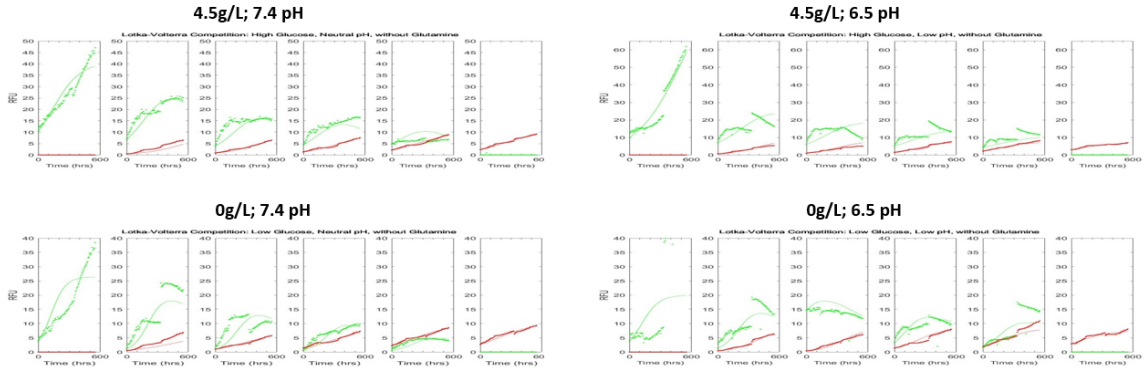

B.

	r_{MCF-7}	$r_{MDA-MB-231}$	K_{MCF-7}	$K_{MDA-MB-231}$	α	β
4.5 g/L Glucose, 7.4 pH, +Glutamine	0.0090083	0.002268243	40.6299239	2479.74226	5.86772365	-190.80898
4.5 g/L Glucose, 7.4 pH, -Glutamine	0.00258612	0.004617902	279.59422	11.5181197	11.9405862	-0.0856875
4.5 g/L Glucose, 6.5 pH, +Glutamine	0.00320443	0.020023245	530.294241	6.29360676	22.2919327	0.10873682
4.5 g/L Glucose, 6.5 pH, -Glutamine	0.00398154	0.008349796	369.570409	6.46236009	43.4810517	0.00420556
0 g/L Glucose, 7.4 pH, +Glutamine	0.01133825	0.002719719	28.3109023	3518.42156	3.41385677	-191.28472
0 g/L Glucose, 7.4 pH, -Glutamine	0.00445318	0.005462004	111.400069	9.63022009	-3.83294222	0.02022454
0 g/L Glucose, 6.5 pH, +Glutamine	0.00529779	0.013626163	28.8414935	6.90636312	0.27455018	0.22164312
0 g/L Glucose, 6.5 pH, -Glutamine	0.02704913	0.009966181	57.0210363	6.9320509	12.2343677	0.00487371

Figure 5: A. Estimation of competition coefficients using OLS fit of Lotka-Volterra competition growth curves. Fluorescence data (RFU) from experiment 2 replicates were averaged and OLS algorithm used to obtain curves. **B.** Estimates of growth rate and carrying capacity reflect previous estimates while

289 estimates of competition coefficients revealed the large competitive effect of MDA-MB-231 on MCF-7
290 cells.

291

292 As before, MCF-7 had higher intrinsic growth rates and carrying capacities than MDA-MB-231 under all 8
293 culture conditions of high/low glucose, high/low pH and presence/absence of glutamine. For all culture
294 conditions, $\alpha > 1$ (as high as 12.6) and $\beta \approx 0$. This indicates that the MDA-MB-231 cells had large
295 competitive effects on MCF-7 growth, and that MCF-7 cells had virtually no inhibitory effects on the
296 growth of MDA-MB-231 cells. These α/β values indicate that the competitive advantage gained by the
297 MDA-MB-231 cells is due primarily to frequency dependent (FD) effects.

298 These effects can also be seen in the slope of the final ten time points of the mixed cultures. Upon the
299 addition of MDA-MB-231 cells, MCF-7 cells show a large decrease in their final slope, even becoming
300 negative, then approaching zero as the starting frequency of MDA-MB-231 cells increases. Conversely,
301 the final slopes of the MDA-MB-231 populations increased in the presence of MCF-7 cells but decreased
302 with the starting frequency of MDA-MB-231 cells, suggesting that these cells were still replacing MCF-7
303 cell at the end of our experiments.

304 The greatest effect of MDA-MB-231 on MCF-7 (highest α) occurred under conditions of 4.5g/L glucose,
305 6.5pH, and glutamine absent conditions. The greatest effect of MCF-7 cells on MDA-MB-231 (highest β)
306 occurred in the absence of glucose and glutamine at neutral pH. This fits our original predictions;
307 however, the effect of β is not strong enough to rescue MCF-7 cells from competitive exclusion. In
308 accordance with the hypothesis that glucose permits MDA-MB-231 cells to be highly competitive, the
309 lowest α's occurred under glucose-starved conditions. Further, both cell types appear to experience
310 decreased growth efficiency and competition in glucose/glutamine starved, and acidic conditions. This is

311 consistent with more general ecological studies showing that competition between species is generally
312 less under harsh physical conditions (41, 42).

313 As expected, MDA-MB-231 experienced the greatest competitive advantage under high glucose,
314 glutamine starved, and acidic conditions. Observations of growth curves at different starting frequencies
315 further confirmed that, although growth of MCF-7 was impacted by starting frequency, under no
316 conditions were they capable of gaining a competitive advantage. In conclusion, only frequency-
317 dependent interactions explain the competitive outcomes seen in the co-culture microspheres.

318 ***In Vivo Confirmation of Competition Outcome***

319 To evaluate whether our results hold *in vivo*, MDA-MB-231 and MCF-7 cells were grown in the
320 mammary fat pads of 8-10 week old nu/nu female mice. Three tumor models were evaluated: only MCF-
321 7, only MDA-MB-231, and 1:1 mix of both cell types with three replicates for each. Tumor volume was
322 measured weekly. At five weeks, the tumors were harvested and evaluated for ER expression which
323 marks MCF-7 (ER positive) cells providing estimates of the ratio of MDA-MB-231 to MCF-7 cells (Figure
324 6)**.**

325

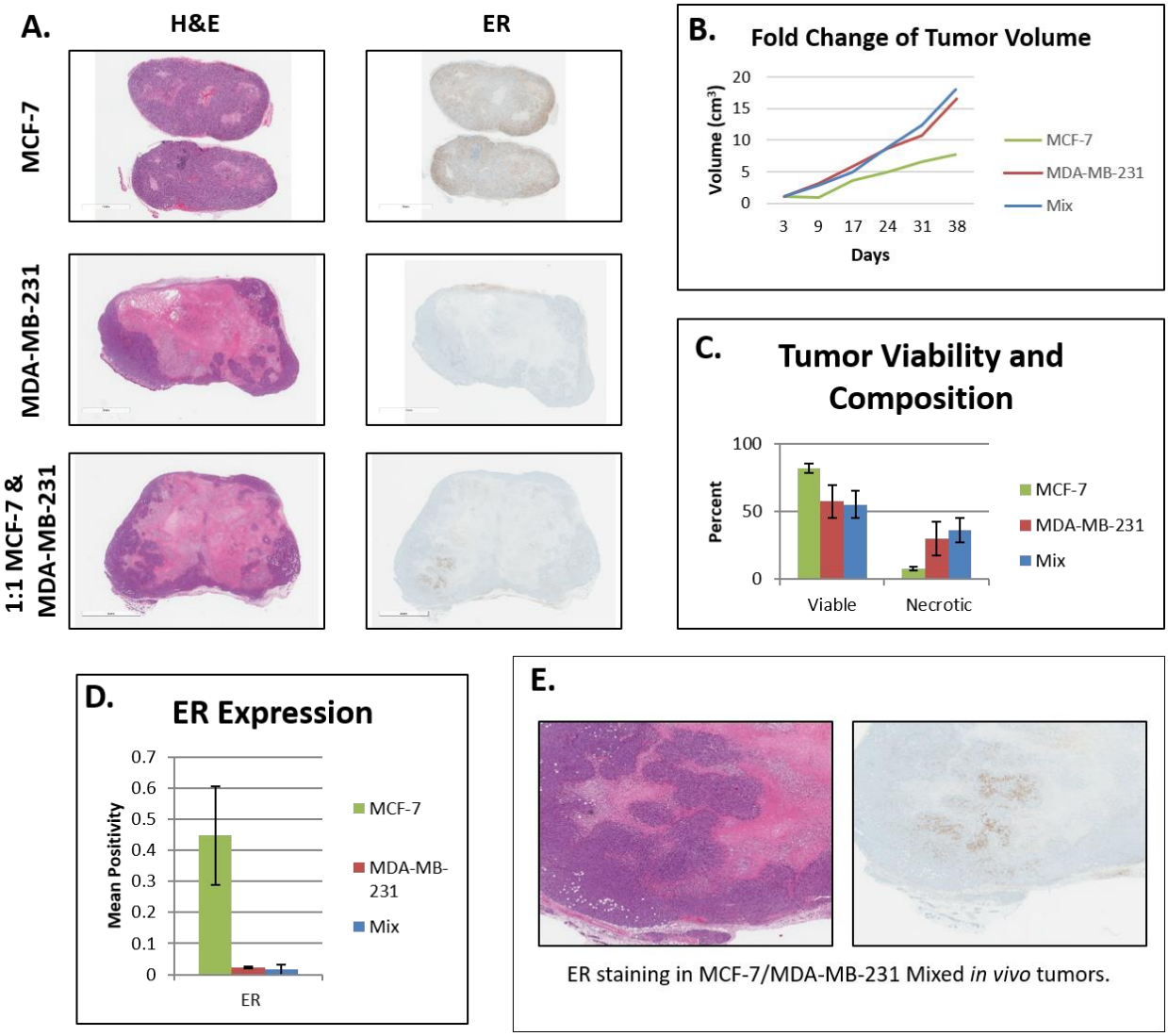

Figure 6: Results of *in vivo* mono- and co- culture tumors. **A.** Histology slides of MCF-7, MDA-MB-231, and 1:1 co-cultured tumors. Slides were stained with H&E and ER immune stain. **B.** Average fold change of tumor volume reflects relative growth. **C.** Tumor viability for all three tumor types. Notice a decrease in viability and increase in necrosis in the MDA-MB-231 and mixed tumors. **D.** Measures of ER biomarker staining for each tumor type. **E.** The presence of small clumps of ER staining in mixed tumors reflect the clumping of MCF-7 cells in the progression of the mixed tumor spheroids. This indicates the eventual elimination of MCF-7 due to competitive inhibition by MDA-MB-231.

335 Changes in tumor size over five weeks indicated that the presence of MDA-MB -231, whether alone or in
336 the presence of MCF-7, resulted in a higher tumor growth rate compared to the MCF-7 only tumors. This
337 suggests that the growth dynamics of the MDA-MB-231 cells gain some advantage *in vivo*. Beyond 24
338 days, it appeared that the mixed tumors grew more rapidly than the MDA-MB-231 monoculture tumors.
339 This suggests that the presence of the competing MCF-7 cell type resulted in less inhibition of the MDA-
340 MB-231 cells *in vivo*. Like the spheroids, MDA-MB-231 cells seem to have higher growth rates as the
341 frequency of MCF-7 cells increases.

342 H&E staining indicated that MCF-7 tumors had the greatest viability and lowest necrosis while MDA-MB-
343 231 tumors displayed decreased viability and increased necrosis. This illustrates the drastic effect that
344 these phenotypes have *in vivo*. The small differences in necrotic and viable tissue between the MDA-
345 MB-231 and mixed tumors are indicative of the expansive effect that MDA-MB-231 phenotype has on
346 tumor progression.

347 ER staining was used to identify the final frequency of MDA-MB-231 and MCF-7 cells. The amount of ER
348 staining in the mixed tumors was comparable to the amount found in the MDA-MB-231 tumor,
349 indicating loss of MCF-7 clones at the experiment's end point. This matches the results from the
350 spheroid experiments demonstrating that MDA-MB-231 cells have a competitive advantage *in vivo* as
351 well. Interestingly, in one of the mixed tumors (shown), we note the presence of clustered ER staining
352 concentrated in an area of interior viable cells. This might reflect the clustering seen in the loss of MCF-7
353 cells in our *in vitro* tumor spheroids.

354

355 **DISCUSSION:**

356 Here we examine competition for resources in cell lines that have been used to represent two
357 phenotypes ("Pioneers" and "Engineers") frequently observed coexisting within the same tumors (4).
358 The "Pioneer" phenotype characteristically exhibits a Warburg metabolic phenotype producing high
359 concentrations of acid in the local microenvironment which promotes invasion and reduces the efficacy
360 of host immune cells. Pioneers are not angiogenic and typically obtain their vascular supply by co-opting
361 host vessels. Thus, they are typically found at the tumor-host interface and exhibit high levels of motility
362 and invasion (43). In contrast, the engineer phenotype is angiogenic, relatively non-invasive with near
363 normal glucose metabolism, and generally localized away from the tumor-host interface (4, 5). While
364 these phenotypes are most commonly found in different regions of the tumor, the eco-evolutionary
365 dynamics that govern their co-existence is not clear. For example, what prevents pioneer cells from
366 invading the engineer population? Similarly, the angiogenic switch is often regarded as a critical step in
367 tumorigenesis but this does not permit the engineer cells to invade the pioneer populations.

368 To understand competition among cancer cell phenotypes within a tumor, we hypothesized that direct
369 competition experiments are critical for understanding factors that may promote or inhibit coexistence.
370 Similar to the classic experiments by Gause (12, 13), we conducted competition experiments between
371 two well-established breast cancer cell lines that exhibit classic phenotypic and in-vivo growth patterns
372 of the 1) "Pioneer" MDA-MB-231 cells, which are highly invasive, non-angiogenic, and glycolytic and the
373 2) "Engineer" MCF-7 cells which are angiogenic, non-invasive, estrogen dependent and have near
374 normal glucose metabolism (4, 5).

375 Our first experiments investigated monocultures in various conditions likely to be present in some
376 regions of an *in vivo* tumor. *In vivo*, MCF-7 tumors generally grow slower than MDA-MB-231 tumors
377 (Figure 6B). Because of this, we were surprised that, in our experimental spheroid model, the growth

378 rate (ri) and carrying capacity (Ki) for MCF-7 cells in monoculture were the same or greater than those of
379 MDA-MB-231 cells under all conditions.

380 We expected these advantages would allow the MCF7 cells to dominate the MDA-MB-231 cells in co-
381 culture. However, the results were entirely opposite to our expectation as the MDA-MB-231 cells
382 became the dominant "species" under all culture conditions and regardless of the initial sizes of the two
383 populations. Indicating the outcomes of interactions between the two populations are almost entirely
384 "frequency dependent". This is reflected in the highly asymmetric and strong competitive effect of
385 MDA-MB-231 cells on MCF-7 cells exhibited by the Lotka-Volterra equations.

386 While the growth rates and carrying capacities of both cell types in monocultures were affected by
387 culture conditions, growth dynamics in co-culture were largely dependent on the presence and
388 frequency of the second cell type. These results highlight the importance of such frequency-dependent
389 dynamics on the progression and outcome of intra-tumoral competition.

390 The magnitude of the competitive effect of one cell type on the other is highly dependent on culture
391 conditions. In spheroids, MDA-MB-231 cells displayed their greatest competitive effect in high glucose
392 and low pH culture conditions while MCF-7 cells, although overall less competitive, showed their
393 greatest competitive effect in low glucose and neutral pH culture conditions. This aligns with the
394 "pioneer" and "engineer" phenotypic patterns and suggests that tumor heterogeneity is driven not only
395 by clonal growth efficiency but also by the landscape of the tumor microenvironment. Because
396 alterations in glucose and pH can significantly affect the competitive ability of different cell phenotypes,
397 manipulation of the microenvironment via therapies could directly influence intra-tumoral evolution and
398 cell-type composition.

399 Our investigation suggests that the competition dynamics observed in tumor spheroids also occur *in*
400 *vivo*. This is evident not only in the outcome of competition between MCF-7 and MDA-MB-231 cells, but

401 also by the spatial patterns observed both *in vivo* and *in vitro*. The emergence of such spatial patterns in
402 vitro suggests that some aspects of intratumoral spatial distribution are the result of cellular phenotypic
403 properties. In co-culture spheroids, MCF-7 cells would form a ring of highly clumped cells away from the
404 spheroids edge. The MDA-MB-231 cells were less clumped and formed the spheroids edge by extending
405 their range outward beyond that of the MCF-7 cells. Similar results have previously identified and
406 characterized in vivo by Ibrahim-Hashim et. al. as an integral factor in the outcome of competition
407 models (5).

408 The competitive superiority of MDA-MB-231 over MCF-7 from our in vitro and in vivo experiments
409 suggests new hypotheses. Several eco-evolutionary mechanisms may be responsible. In the competition
410 experiments, the cancer cells experienced pulsed resource renewal every 3-4 days. Thus, over a four day
411 period the culture media likely went from nutrient rich to poor, while metabolite concentrations,
412 including acid, increased (44). In both natural and malignant ecosystems, oscillating resources and
413 metabolites favor traits of 1) "priority", 2) speed, and 3) efficiency (45-48).

414 Here, *priority* is defined by the ability to localize, move to, and invade areas of high resource availability.
415 The higher motility and invasiveness of the MDA-MB-231 allowed them to occupy the outer margins of
416 the spheroid where nutrient concentrations would be highest (5, 29, 32, 49). *Speed* is defined by the
417 rate at which an organism can forage. A high speed allows an organism to pre-empt other organisms via
418 interference with uptake by competitors (50). The high glycolytic capacity of the MDA-MB-231 permits
419 them to acquire glucose faster than their MCF-7 competitors on a per cell basis. Furthermore, MDA-MB-
420 231 do not adhere to each other as the MCF-7 cells did. This gives the MDA-MB-231 a higher surface
421 area for nutrient uptake and less cell-to-cell interference in nutrient uptake. Finally, the motility and
422 speed of nutrient uptake may both contribute to rapid but inefficient foraging. High speed and efficiency
423 benefit the cell both through acquisition of resources and by making them unavailable to its

424 competitors. However, high motility and speed of nutrient uptake often result in rapid but inefficient
425 foraging. The lower intrinsic growth rates and carrying capacities of MDA-MB-231 are consistent with
426 this. *Efficiency* is the capacity of an organism to cheaply and profitably exploit resources when they are
427 scarce. The MCF-7 may be slower, more efficient foragers thus depleting nutrients following the pulse
428 more slowly but in a manner that allowed for greater per cell survival and proliferation, thus explaining
429 their higher growth rates and carrying capacity when grown in mono-culture (51).

430

431 **CONCLUSIONS**

432 Mixed-culture competition experiments in spheroids can successfully track competitive outcomes
433 between cell lines of interest. Such experiments in spheroids may be valuable for quantifying the costs
434 of resistance. Experiments could consider competing a resistant cell line against its sensitive parental
435 cell line under conditions of no therapy (sensitive would be expected to outcompete the resistant cell
436 line) and under conditions of therapy (resistant should outcompete the sensitive cell line). As
437 accomplished here, one could determine differences in growth rates, carrying capacities and
438 competition coefficients. These metrics would be valuable for informing adaptive therapy trials that
439 modulate therapy so as to maintain a population of sensitive cells as a means for competitively
440 suppressing the resistant cells (52-54).

441 Mixed culture competition experiments demonstrate how both the densities and the frequencies of cell
442 types influence the growth rates and population dynamics of cancer cells. Measurements of resource
443 availability and carrying capacities determine limits to growth. The extent to which inter-specific
444 competition coefficients differ significantly from 1, reveal the extent to which cancer cells engage in eco-
445 evolutionary games where the success of a given cancer cell depends both on its phenotype but the
446 phenotypes of the other cancer cells (55-58). Such understanding of how cancer cell types respond to
447 each other and to therapy will be crucial to evolutionarily informed therapies that aim to anticipate and
448 steer the cancer's eco-evolutionary dynamics (59).

449 **METHODS:**

450 ***Cell Culture and acid adaptation in vitro***

451 MCF-7 and MDA-MB-231 cells were acquired from American Type Culture Collection (ATCC, Manassas,
452 VA, 2007–2010) and were maintained in DMEM-F12 (Life Technologies) supplemented with 10% FBS
453 (HyClone Laboratories). Cells were tested for mycoplasma contamination and authenticated using short
454 tandem repeat (STR) DNA typing according to ATCC guidelines. Growth media was supplemented to
455 contain adjusted glucose and glutamine concentrations, depending on desired environmental
456 conditions. Media was also supplemented with 25 mmol/L each of PIPES and HEPES to increase the
457 buffering capacity of the media and the pH adjusted to 7.4 or 6.5 for each spheroid growth condition.

458 ***Transfection (GFP/RFP plasmids)***

459 To establish stable cell lines, the MCF-7 and MDA-MB-231 cells were infected with Plasmids expressing
460 RFP or GFP using Fugene 6 (Promega) at an early passage and were selected using 2 µg/ml puromycin
461 (Sigma).

462 ***3D spheroid co-culture***

463 Perfecta3®96-Well Hanging Drop Plates or non-adhesive U shape bottom 96 well plates were used to
464 grow the primary spheres containing 10,000 or 20,000 total cells. For each experimental condition, the
465 ratio between MCF-7-GFP and MDA-mb-231-RFP was from 0 to 100 percent as follows: 0/100, 20/80,
466 40/60, 60/40, 80/20, 100/0. Each ratio had four replicates for each experiment. An incucyte microscope
467 kept at 37°C and 5% CO2 was used to image the spheroid growth over approximately 30 days. Images
468 and fluorescent intensity were analyzed in Incucyte built-in software and image J. Relative fluorescent
469 units (RFUs) were normalized by averaging red/green fluorescence when the corresponding cell type
470 was absent then subtracting this value from other fluorescent values of that cell type.

471 ***Experimental conditions:***

472 Two experiments were conducted. The first consisted of spheroids with a starting density of 20,000 cells
473 under conditions of high (4.5g/L), medium (2g/L), intermediate (1g/L) and no glucose fully crossed with
474 physiological (7.4) and low (6.5) pH. Spheroids were allowed to grow for roughly 670 hours with
475 fluorescence measured every 24-72 hours. Relative fluorescent units (RFUs) were used to generate
476 estimates of growth rates and carrying capacities.

477 Observations from these spheroids prompted us to conduct a second set of experiments consisting of
478 spheroids with a lower starting density (10,000 cells) cultured under the extremes of nutrient
479 concentration (0 g/L and 4.5 g/L glucose) fully crossed with physiological and low pH. Resilience of
480 growth under no glucose prompted a repeat of the experiment (0 g/L and 4.5 g/L glucose fully crossed
481 with physiological and low pH) with medium lacking glutamine. To improve accuracy of model-fitting,
482 fluorescent values were collected every 6 or 12 hours. These spheroids were also compared using three-
483 way ANOVAs (Ph, nutrient level and starting frequency of cells as independent variables). Additionally,
484 mechanism of growth was determined by fitting growth models as described below.

485 ***Calculation of growth rate and carrying capacity:***

486 Growth rates were calculated as the log change of the first 72 hours after plating. Growth rates were
487 calculated from mono-cultures only. Carrying capacities were calculated as the mean fluorescence of
488 the final ten time points for each experiment. Since their values were similar regardless of starting
489 frequency, and since they dominated the tumor spheroid in all experiments, we could estimate the
490 carrying capacities of MDA-MB-231 cells using all cultures with a starting frequency of $\geq$ 20% MDA-MB-
491 231. Due to competitive effects, MCF-7 carrying capacities were estimated using only the 100% MCF-7
492 spheroids.

493 ***Testing among growth models:***

494 The Ordinary Least Squares (OLS) fitting algorithm was used to fit exponential, Monod-like, Lotka-
495 Volterra, and Gompertz growth models to all monoculture spheroids in experiment 2. Fits were
496 performed by allowing adjustment of all input parameters. This provided the best fits (highest adjusted
497 R^2, lowest RMSE). Estimates of growth rates and carrying capacities obtained this way were very close to
498 our original estimates, providing further validity.

499 ***Competition Coefficient Estimation:***

500 For each culture condition in experiment 2, fluorescent values were averaged across the four
501 experimental replicates. OLS fitting was used with no initial guess for growth rate or carrying capacity.
502 All plotting, optimization, and analysis was performed using MATLAB.

503 ***In Vivo Tumor Culture:***

504 MCF7 and MDA-MB-231 breast cancer cell lines were purchased from ATCC. Both cells were
505 authenticated by short tandem repeat analysis and tested for mycoplasma. Xenograft studies were
506 performed by the guidelines of the IACUC of the H. Lee Moffitt Cancer Center using eight- to ten-week-
507 old female nu/nu mice (Envigo). Mice had free access to water and food for the whole duration of the
508 experiment. For MDA-MB-231 and MCF7 mono-tumor formation, 10 million cells were injected into
509 cleared mammary fat pads as described previously (4). For mixed cultures, a 1:1 mixture of 5 million
510 MDA-MB231 and 5 million MCF7 cells were injected. One week before cell injection, an estrogen pellet
511 (0.72 mg slow-release, Innovative Research of America) was implanted to allow for the growth of ER-
512 positive MCF7 tumors. Five weeks later, tumors were harvested.

513

514

1. Gillies RJ, Brown JS, Anderson AR, Gatenby RA. Eco-evolutionary causes and consequences of temporal changes in intratumoural blood flow. Nature Reviews Cancer. 2018;18(9):576-85.
2. Galon J, Costes A, Sanchez-Cabo F, Kirilovsky A, Mlecnik B, Lagorce-Pagès C, et al. Type, density, and location of immune cells within human colorectal tumors predict clinical outcome. Science. 2006;313(5795):1960-4.
3. Galon J, Mlecnik B, Bindea G, Angell HK, Berger A, Lagorce C, et al. Towards the introduction of the 'Immunoscore'in the classification of malignant tumours. The Journal of pathology. 2014;232(2):199-209.
4. Lloyd MC, Cunningham JJ, Bui MM, Gillies RJ, Brown JS, Gatenby RA. Darwinian dynamics of intratumoral heterogeneity: not solely random mutations but also variable environmental selection forces. Cancer research. 2016:canres. 2962.015.
5. Ibrahim-Hashim A, Robertson-Tessi M, Enriquez-Navas PM, Damaghi M, Balagurunathan Y, Wojtkowiak JW, et al. Defining cancer subpopulations by adaptive strategies rather than molecular properties provides novel insights into intratumoral evolution. Cancer research. 2017;77(9):2242-54.
6. Gerlinger M, Rowan AJ, Horswell S, Larkin J, Endesfelder D, Gronroos E, et al. Intratumor heterogeneity and branched evolution revealed by multiregion sequencing. New England journal of medicine. 2012;366(10):883-92.
7. Polyak K. Heterogeneity in breast cancer. The Journal of clinical investigation. 2011;121(10):3786-8.
8. Perou CM, Sørlie T, Eisen MB, Van De Rijn M, Jeffrey SS, Rees CA, et al. Molecular portraits of human breast tumours. Nature. 2000;406(6797):747.
9. Robinson SP, Jordan VC. The paracrine stimulation of MCF-7 cells by MDA-MB-231 cells: possible role in antiestrogen failure. European Journal of Cancer and Clinical Oncology. 1989;25(3):493-7.
10. Lotka AJ. Contribution to the theory of periodic reactions. The Journal of Physical Chemistry. 1910;14(3):271-4.
11. Volterra V. Variazioni e fluttuazioni del numero d'individui in specie animali conviventi: C. Ferrari; 1927.
12. Gause G. The struggle for existence, 163 pp. Williams and Wilkins, Baltimore. 1934.
13. Gause G, Witt A. Behavior of Mixed Populations and the Problem of Natural Selection. The American Naturalist. 1935;69(725):569-609.
14. Barker J, Podger R. Interspecific competition between Drosophila melanogaster and Drosophila simulans: effects of larval density on viability, developmental period and adult body weight. Ecology. 1970;51(2):170-89.
15. Park T. Experimental studies of interspecies competition II. Temperature, humidity, and competition in two species of Tribolium. Physiological Zoology. 1954;27(3):177-238.
16. De Wit C, Van den Bergh J. Competition between herbage plants. Journal of Agricultural Science. 1965;13:212-21.
17. Kimmerling RJ, Prakadan SM, Gupta AJ, Calistri NL, Stevens MM, Olcum S, et al. Linking single-cell measurements of mass, growth rate, and gene expression. Genome biology. 2018;19(1):207.
18. Gerstein AC, Otto SP. Cryptic fitness advantage: diploids invade haploid populations despite lacking any apparent advantage as measured by standard fitness assays. PloS one. 2011;6(12):e26599.
19. Hart T, Chandrashekhar M, Aregger M, Steinhart Z, Brown KR, MacLeod G, et al. High-resolution CRISPR screens reveal fitness genes and genotype-specific cancer liabilities. Cell. 2015;163(6):1515-26.
20. Gallaher J, Brown J, Anderson ARA. The dynamic tumor ecosystem: how cell turnover and trade-offs affect cancer evolution. bioRxiv. 2018:270900.
21. Kaznatcheev A, Peacock J, Basanta D, Marusyk A, Scott JG. Fibroblasts and Alectinib switch the evolutionary games played by non-small cell lung cancer. bioRxiv. 2018:179259.

562 22. Holliday DL, Speirs V. Choosing the right cell line for breast cancer research. Breast cancer
563 research. 2011;13(4):215.
564 23. Neve RM, Chin K, Fridlyand J, Yeh J, Baehner FL, Fevr T, et al. A collection of breast cancer cell
565 lines for the study of functionally distinct cancer subtypes. Cancer cell. 2006;10(6):515-27.
566 24. Kao J, Salari K, Bocanegra M, Choi Y-L, Girard L, Gandhi J, et al. Molecular profiling of breast
567 cancer cell lines defines relevant tumor models and provides a resource for cancer gene discovery. PloS
568 one. 2009;4(7):e6146.
569 25. Horwitz K, Costlow M, McGuire W. MCF-7: a human breast cancer cell line with estrogen,
570 androgen, progesterone, and glucocorticoid receptors. Steroids. 1975;26(6):785-95.
571 26. Levenson AS, Jordan VC. MCF-7: the first hormone-responsive breast cancer cell line. Cancer
572 research. 1997;57(15):3071-8.
573 27. Sutherland RM, McCredie JA, Inch WR. Growth of multicell spheroids in tissue culture as a model
574 of nodular carcinomas. Journal of the National Cancer Institute. 1971;46(1):113-20.
575 28. Sutherland RM. Importance of critical metabolites and cellular interactions in the biology of
576 microregions of tumors. Cancer. 1986;58(8):1668-80.
577 29. Sutherland RM. Cell and environment interactions in tumor microregions: the multicell spheroid
578 model. Science. 1988;240(4849):177-84.
579 30. Tofilon PJ, Arundel CM, Deen DF. Response to BCNU of spheroids grown from mixtures of drug-
580 sensitive and drug-resistant cells. Cancer chemotherapy and pharmacology. 1987;20(2):89-95.
581 31. Beaupain R. A method for three-dimensional coculture of cancer cells combined to any other
582 type of cells maintained organotypically. Methods in cell science. 1999;21(1):25-30.
583 32. Hirschhaeuser F, Menne H, Dittfeld C, West J, Mueller-Klieser W, Kunz-Schughart LA.
584 Multicellular tumor spheroids: an underestimated tool is catching up again. Journal of biotechnology.
585 2010;148(1):3-15.
586 33. Weiswald L-B, Bellet D, Dangles-Marie V. Spherical cancer models in tumor biology. Neoplasia.
587 2015;17(1):1-15.
588 34. Damaghi M, Gillies R. Phenotypic changes of acid-adapted cancer cells push them toward
589 aggressiveness in their evolution in the tumor microenvironment. Cell Cycle. 2017;16(19):1739-43.
590 35. Benzekry S, Lamont C, Beheshti A, Tracz A, Ebos JM, Hlatky L, et al. Classical mathematical
591 models for description and prediction of experimental tumor growth. PLoS computational biology.
592 2014;10(8):e1003800.
593 36. Marušić M, Bajzer Ž, Freyer J, Vuk-Pavlović S. Analysis of growth of multicellular tumour
594 spheroids by mathematical models. Cell proliferation. 1994;27(2):73-94.
595 37. Malthus TR. An Essay on the Principle of Population1872.
596 38. Kucharavy D, De Guio R. Application of logistic growth curve. Procedia engineering.
597 2015;131:280-90.
598 39. Casey AE. The experimental alteration of malignancy with an homologous mammalian tumor
599 material: I. Results with intratesticular inoculation. The American Journal of Cancer. 1934;21(4):760-75.
600 40. Monod J. The growth of bacterial cultures. Annual review of microbiology. 1949;3(1):371-94.
601 41. Liancourt P, Callaway RM, Michalet R. Stress tolerance and competitive-response ability
602 determine the outcome of biotic interactions. Ecology. 2005;86(6):1611-8.
603 42. Douda J, Doudová J, Hulík J, Havrdová A, Boublík K. Reduced competition enhances community
604 temporal stability under conditions of increasing environmental stress. Ecology. 2018;99(10):2207-16.
605 43. Wells A, Grahovac J, Wheeler S, Ma B, Lauffenburger D. Targeting tumor cell motility as a
606 strategy against invasion and metastasis. Trends in pharmacological sciences. 2013;34(5):283-9.
607 44. Hulikova A, Vaughan-Jones RD, Swietach P. Dual role of CO2/HCO3− buffer in the regulation of
608 intracellular pH of three-dimensional tumor growths. Journal of Biological Chemistry.
609 2011;286(16):13815-26.

45. Amend SR, Gatenby RA, Pienta KJ, Brown JS. Cancer foraging ecology: Diet choice, patch use, and habitat selection of cancer cells. Current Pathobiology Reports. 2018;6(4):209-18.
46. Brown JS. Coexistence on a seasonal resource. The American Naturalist. 1989;133(2):168-82.
47. Chesson P, Gebauer RL, Schwinning S, Huntly N, Wiegand K, Ernest MS, et al. Resource pulses, species interactions, and diversity maintenance in arid and semi-arid environments. Oecologia. 2004;141(2):236-53.
48. Hagy HM, Kaminski RM. Determination of foraging thresholds and effects of application on energetic carrying capacity for waterfowl. PLoS One. 2015;10(3).
49. Mueller-Klieser W, Freyer J, Sutherland R. Influence of glucose and oxygen supply conditions on the oxygenation of multicellular spheroids. British journal of cancer. 1986;53(3):345.
50. Richards SA, Nisbet RM, Wilson WG, Possingham HP. Grazers and diggers: exploitation competition and coexistence among foragers with different feeding strategies on a single resource. The American Naturalist. 2000;155(2):266-79.
51. Taylor TB, Wass AV, Johnson LJ, Dash P. Resource competition promotes tumour expansion in experimentally evolved cancer. BMC evolutionary biology. 2017;17(1):268.
52. Gatenby RA, Silva AS, Gillies RJ, Frieden BR. Adaptive therapy. Cancer research. 2009;69(11):4894-903.
53. Gallaher JA, Enriquez-Navas PM, Luddy KA, Gatenby RA, Anderson AR. Spatial heterogeneity and evolutionary dynamics modulate time to recurrence in continuous and adaptive cancer therapies. Cancer research. 2018;78(8):2127-39.
54. Zhang J, Cunningham JJ, Brown JS, Gatenby RA. Integrating evolutionary dynamics into treatment of metastatic castrate-resistant prostate cancer. Nature communications. 2017;8(1):1816.
55. Basanta D, Simon M, Hatzikirou H, Deutsch A. Evolutionary game theory elucidates the role of glycolysis in glioma progression and invasion. Cell proliferation. 2008;41(6):980-7.
56. Archetti M. Evolutionary game theory of growth factor production: implications for tumour heterogeneity and resistance to therapies. British journal of cancer. 2013;109(4):1056-62.
57. Gatenby RA, Vincent TL. Application of quantitative models from population biology and evolutionary game theory to tumor therapeutic strategies. Molecular cancer therapeutics. 2003;2(9):919-27.
58. Brown JS. Why Darwin would have loved evolutionary game theory. Proceedings of the Royal Society B: Biological Sciences. 2016;283(1838):20160847.
59. Staňková K, Brown JS, Dalton WS, Gatenby RA. Optimizing cancer treatment using game theory: A review. JAMA oncology. 2019;5(1):96-103.

ACKNOWLEDGEMENTS:

We thank Jeffrey West for assistance with coding, we thank Chris Whelan and Dorothy Wallace for discussion and good ideas. Funding was provided by NIH/NCI 1U54CA193489-01A1, Cancer as a Complex Adaptive System, NIH/NCI U54 Supplement, The tumor-host evolutionary arms race, and R01 CA077575. This work was supported in part by the Analytic Microscopy Core Facility and the Tissue Core Facility at the H. Lee Moffitt Cancer Center & Research Institute; an NCI designated Comprehensive Cancer Center (P30-CA076292).

AUTHOR CONTRIBUTIONS:

All authors participated in the study ideas and the writing of the paper. M.D., A.I., A.R.F. and J.S.B designed the experiments. M.D., A.I. and A.R.F. collected the data. A.R.F., J.J.C. and J.S.B. performed the statistical analyses.

COMPETING INTERESTS:

The authors declare no competing financial interests.